Marko Švaco
Bojan Jerbić
Filip Šuligoj

ISSN 1333-1124
eISSN 1849-1391

AUTONOMOUS ROBOT LEARNING MODEL BASED ON VISUAL INTERPRETATION OF SPATIAL STRUCTURES

UDC 681.51:004.032.26

Summary

The main concept of the presented research is an autonomous robot learning model for which a novel ARTgrid neural network architecture for the classification of spatial structures is used. The motivation scenario includes incremental unsupervised learning which is mainly based on discrete spatial structure changes recognized by the robot vision system. The learning policy problem is presented as a classification problem for which the adaptive resonance theory (ART) concept is implemented. The methodology and architecture of the autonomous robot learning model with preliminary results are presented. A computer simulation was performed with four input sets containing 22, 45, 73, and 111 random spatial structures. The ARTgrid shows a fairly high (>85%) match score when applied with already learned patterns after the first learning cycle, and a score of >95% after the second cycle. Regarding the category proliferation, the results are compared with a more predictive modified cluster centre seeking algorithm.

Key words: *Autonomous systems, Machine learning, Adaptive Resonance Theory*

1. Introduction

Development of any technical system assumes the attention attributed to autonomous capabilities. Usually it means to understanding the effect of the environment and to learning based on experience. The main problems, which roboticists are facing, are control and behaviour of robot models. Within this area of research, efforts are made to enable robots to work autonomously and act in changing, dynamic and unpredictable environmental conditions. A detailed overview of ongoing research is presented in Section 2. The main hypothesis is that autonomous learning occurs in response to the visual cognition and interpretation of objects and their arrangement in the environment. Autonomous learning of the dynamic input space includes retaining, classifying and organizing the knowledge associated with complex actions. Through visual interaction and demonstration it is possible to transfer the knowledge about a particular problem to the robot. The robot autonomously encodes the environment state and the dynamic spatial arrangement of objects. Human interpretation of the environment (workspace) is mainly based on the context and, more precisely, on the structural arrangement of objects and their respective meaning. The industrial process of product assembly can be considered as an example. A person can intuitively connect arbitrarily spaced mounting elements in the workspace, bringing them into mutual spatial and geometrical relationship. The process is carried out by precisely executing a defined sequence of actions required to build the final product. Another example could be taken from medical practice, i.e. from surgical procedures. A defined collection of surgical instruments, objects and tools in the operating theatre indicates a specific surgery procedure. It also specifies a series of actions and the manipulation of individual instruments that the appropriate surgery procedure requires. These quite different examples clearly demonstrate that by observing a limited working domain, we can make certain assumptions about the set of actions, i.e. about the behaviour associated with the current arrangement and meaning of objects in the workspace.

Robot behaviour can be described as sensorimotor mapping from the perceptual space to the activity space. The hypothesis proposed in this paper is that similar situations (stimuli) trigger similar complex actions (behaviour). Thus, the action and perceptual space can be classified. A robotic system should be capable of observing, mapping and finally learning dynamic changes in the object spatial layout within the work environment. The most important step in this complex process is the learning ability which will be attributed by the developed ARTgrid classification architecture [1]. The ARTgrid architecture is based on ART (Adaptive Resonance Theory) universal coding mechanisms [2, 3]. ART is a cognitive neural theory which attempts to explain how a technical system, motivated by biological paradigms, can autonomously learn, categorize, recognize and predict events in a dynamic environment. A series of well-established artificial neural networks (ANN) were steadily developed following basic ART principles. ART networks are implemented for both the supervised and the unsupervised classification and clustering. Furthermore, adaptive resonance theory was developed to avoid the stability-plasticity dilemma in competitive networks defined by Grossberg [2]. The stability-plasticity dilemma addresses the problem of how a learning system can preserve its previously acquired knowledge while keeping the ability of learning new input patterns [4]. Plasticity denotes successful adaptation to changing conditions in the environment and the learning of new input patterns. The stability of ART can be characterized through the ability of learning new input patterns without "forgetting" previous ones. For the purpose of learning a new behaviour policy, by a robot, both characteristics are equally important and cannot be analysed separately. The approach proposed in this paper is different from ART neural networks found in literature because it enables both the classification of spatial structures based on their shape (morphology) and the arrangement of individual objects within spatial structures.

The rest of the paper is organized as follows. Section 2 gives an overview of related research. Section 3 presents the motivation and a use case scenario around which simulations are conducted. In Section 4, the architecture of the developed learning model based on the ARTgrid neural network is presented. Section 5 gives an extensive overview of various simulations that were conducted. Section 6 presents the discussion of the results and conclusions, and the final section, Section 7, highlights the future work.

2. Related work

An autonomous robot [5, 6] is a device with certain motor skills and sensors which provide feedback from the dynamic environment with which the robot is in continuous interaction. It is an intelligent and, to a certain extent, a self-sufficient machine that can operate in a real world environment without explicit human control. An example of an actual autonomous robot system can be noted within the probabilistic model of industrial robot group control developed in [7] and a multiagent robotic system developed in [8]. Research considering the development of behaviour policy learning based on the environment perception and industrial assembly processes is described in [9 - 15]. The research carried out in [9] deals with the environment modelling and artificial cognition mechanisms of robotic manufacturing systems. The main goal of the research is to enable effective information acquisition for the purpose of adequate reasoning and learning. In [10], a model for behaviour policy learning based on the learning by demonstration paradigm was developed. The study is based on learning new assembly processes through virtual reality. The model takes into account the state (position, orientation, process) of individual objects without considering the overall structure of the product. Newly acquired behaviour policies are then used in similar assembly processes. Paul et al. [11] developed a model of behaviour policy learning through the observation of human actions. The actions that the system recognizes consist of grasp, push, and fine motion. The main focus of the research is the recognition of mutual object dependencies and the type of contact at different levels of granularity. A related research [12] utilizes multimodal behaviour policy learning based on the physical human-robot interaction. Learned behaviour patterns can be used for identical problem cases without a possibility for later generalizations. Lenz et al. [13, 14] verify the research on an industrial robotic setup by learning new tasks through interaction based on multi-modal inputs. Learning is based on decomposing the task into working structure primitives. A collaboration and learning scenario in a simplified recreation of spatial structures is presented in [15]. Both approaches tend to have a predefined number of composites.

Machine learning algorithms from the family of ART neural networks find their applications in a variety of technical fields [16] and particularly in robotics [17, 18]. ART is mainly utilized to overcome the problem of incremental learning and self-organization of knowledge in the process of supervised and unsupervised learning. The selected literature [2 - 3], covers the fundamentals of adaptive resonance theory and explains basic concepts and functionalities of the ART. Research described in [17 - 21] implemented and developed specific ART architectures for pattern recognition and learning within the robotic domain. In [19], a modified fuzzy ARTMAP architecture was used for industrial robot complex pattern learning in manipulation and assembly processes. The complex action pattern is reduced to a set of basic actions interpreted by the robot. The research is related to the creation of self-adapting robots capable of incremental and dynamic behaviour policy learning, mainly manipulation skills. The proposed model is implemented as a neural network robot controller (NNC). Authors in [20] used the analogue ART-2 architecture for cross-modality learning both for the recognition and the learning of human gestures. That architecture was applied to a humanoid robotic platform. The process of learning utilizes multiple input modalities such as sound, gestures, and visual interpretation of the environment. In a related study, [21], a supervised ARTMAP artificial neural network was implemented in order to recognize gestures that uniquely describe dynamic spatial structures. A gesture can be closely correlated with a spatial structure. The authors define gestures as a function of time and position of the human hand. A specific meaning is associated with each gesture illustrating the robot behaviour policy learning. Certain mechanisms adopted from game theory [22] can improve the categorization of ART networks. One of the main issues in ART is an increase in memory requirements through time and an accurate specification of learning tasks. An adaptive classification and clusterization method based on the Nash Equilibrium is proposed. Continuous optimization of the vigilance parameter is performed, with a direct impact on the total number of output categories and their respective sizes. Tan et al. [23] propose a unified ART based framework for learning by association and matching, called Fusion ART. Fusion ART is also capable of learning multi-modal inputs by instruction and reinforcement. The architecture is developed for acquiring knowledge through multi-dimensional mappings, where each map is associated with a distinctive ART layer.

The main problem with the quoted related literature is that there is no specific architecture that would provide a sufficiently developed mechanism for dealing with the spatial structure morphology, arrangement of individual objects within these structures and their respective learning. This paper addresses the fore mentioned issues, giving a detailed overview of the developed learning model based on the ARTgrid neural network.

3. Motivation and use case scenario

As depicted in Fig.1a, a robot, i.e. the learning agent, collects information from the environment. It processes the information, reasons and makes decisions upon which it acts on the environment. Interaction with the environment is imperative for reasoning about a certain object or event. The main hypothesis is that similar stimuli activate a related set of actions. A similar stimulus, i.e. a similar spatial structure, can be defined when individual objects form similar spatial relations, when they are slightly translated or rotated, or when they differ in shape slightly. In Fig.1b, a global view of the use case motivation scenario is presented. An autonomous agent (AA), either a human or a robot agent, is acting in the environment. The main purpose of this agent is to transfer information and knowledge about the spatial structures and the arrangement of individual objects within the structure to the learning agent. The autonomous agent can either be a human who is transferring her/his knowledge to the learning agent or another robot already equipped with a certain set of skills.

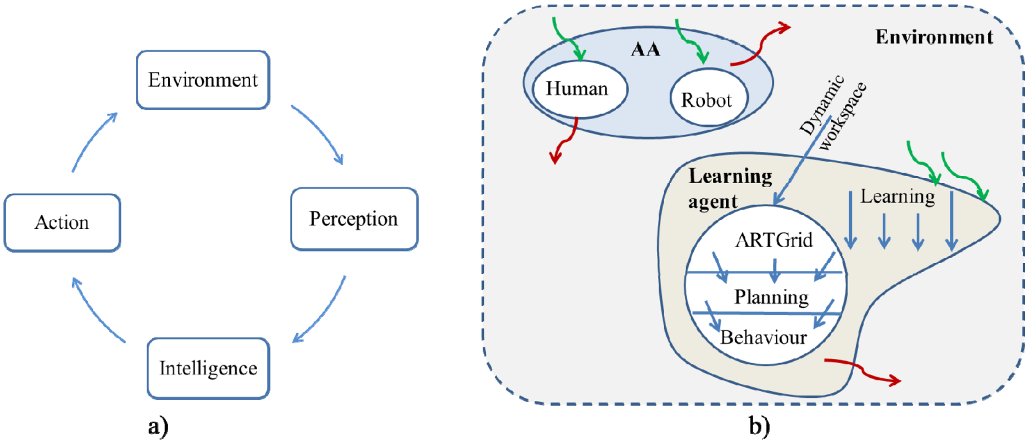

Fig. 1 a) The general sequence of information and action within an interaction scenario b) Proposed general model of learning through visual interaction within a dynamic workspace –outgoing (red) arrows indicate actions, incoming (green) indicate information retrieval from the environment

On the other hand, the general model of the learning agent is proposed as a three component system consisting of a learning, a planning, and a behaviour module. The planning module developed in the earlier research [24], used for action planning in a multiagent robotic system, could be adopted for the future development of a single agent planning module. In this paper, the learning component will be described in detail. The use case scenario consists of the blocks world used for assembly, as depicted in Fig. 2. The main idea of the proposed research is that the robot (Fig. 2) will assemble previously learned spatial structures from an unordered set of objects.

4. Robot learning model: ARTgrid

In the use case scenario the autonomous agent uses visual demonstrations of a particular assembly process. Perception and recognition capabilities of the learning agent are encompassed by the ARTgrid learning module within the general model. Objects in the robot workspace form a certain spatial structure.

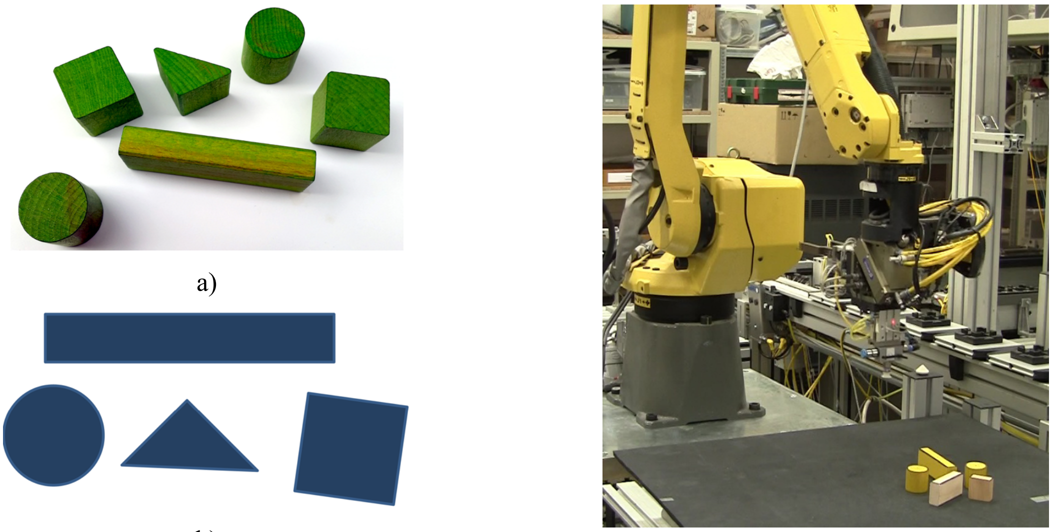

a) b) c)

Fig. 2 a) Actual objects in the blocks world b) virtual objects used for simulation and verification purposes c) the actual robot where the learning model will be applied

A spatial structure can be defined at two levels of granularity. First, the morphology, i.e. the general shape can be recorded without regarding individual objects in the structure. At a more detailed level, for providing finer details, individual objects and their respective information are obtained (position, orientation). The generalization capability of the proposed ANN is important for providing the learning agent information about solving new but similar tasks. A spatial structure is recognized in two-dimensional space in which objects form different spatial relationships with expected different meanings.

Let $\mathbf{I}_g = (I_{g_{11}}, I_{g_{12}}, \ldots, I_{g_{mn}})$ $g \in [1, Np]$ denote the acquired input structure where $\mathbf{I}_{g_{ij}} \in [0,1]$. Let $\mathbf{W}_j$ denote the connection weight matrix. ARTgrid main parameters include a learning rate parameter $\beta_i \in [0,1]$, and a vigilance parameter $\rho_i \in [0,1]$.

Learning laws utilized within the ARTgrid model are introduced into (1) and (2). The first equation uses the learning law from the original fuzzyART algorithm [25], where the connection weights only decrease or remain at the same values. No increase is possible, i.e. certain characteristics applied to the network numerous times cannot be "coded" if they have not existed in the prototype vector (i.e. prototype spatial structure). For that reason, a learning law used in the previous research [26] is applied as shown in (2). Utilizing (2) the weights can both increase and decrease in proportion to the similarity with the applied input structure. Fast learning is demonstrated in (3), which accounts for the direct replication of the input pattern within the output neuron when a new output category is formed.

$$\mathbf{W}_{\mathrm{j}}^{(\mathrm{t})} = \beta(\mathbf{I} \wedge \mathbf{W}_{\mathrm{j}}^{(\mathrm{t-1})}) + (1-\beta)\mathbf{W}_{\mathrm{j}}^{(\mathrm{t-1})} \tag{1}$$

$$\mathbf{W}_{\mathrm{j}}^{(\mathrm{t})} = \beta(\mathbf{I}) + (1-\beta)\mathbf{W}_{\mathrm{j}}^{(\mathrm{t-1})} \tag{2}$$

$$\mathbf{W}_{\mathrm{j}}^{(\mathrm{t})} = \mathbf{I} \wedge \mathbf{W}_{\mathrm{j}}^{(\mathrm{t-1})} \tag{3}$$

The fuzzy AND operator $\wedge$ is defined as $(\mathbf{A} \wedge \mathbf{B})_{ij} \equiv \min(A_{ij}, B_{ij})$, the fuzzy OR operator $\vee$ is defined $(\mathbf{A} \vee \mathbf{B})_{ij} \equiv \max(A_{ij}, B_{ij})$, for the matrices $\mathbf{A}$ and $\mathbf{B}$.

4.1 ARTgrid hierarchy and organization

The ARTgrid neural network is organized in two hierarchical levels - the Ga1 and the Ga2 level as depicted in Fig. 3. The Ga1 level records only certain features of the input spatial structures providing a more generalized method for category recognition. Within each Ga1 level, there exist a certain (dynamically increasing) number of related categories coded in the Ga2 level. Each Ga1 category consists of at least one Ga2 category. Ga2 categories represent more specific forms of inputs passed into the parent Ga1 category. The input structure is recognized at output neurons in Ga1. When a certain output neuron in Ga1 is in resonance, it triggers an output to an associated category in Ga2. A secondary match tracking and resonance process follows, where the attentional and the orienting subsystem are activated within Ga2.

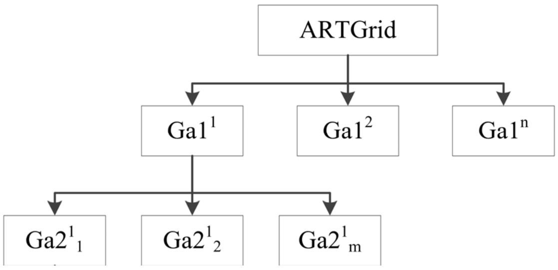

Fig. 3 Architecture of the ARTgrid ANN

Furthermore, each Ga2 category has an associated object matrix (MTO). It is not possible to detect all applied objects within the output Ga1 class by only inspecting the morphology, i.e. the structure shape. The main dissimilarity comes from individual objects that cannot be detected from the fused structure. The object matrix describes the activity of individual objects in the output class structure. As new inputs are applied to the output class, both the structure and the MTO (Table 1) are modified given the learning rule in (2).

Table 1 MTO (object matrix) associated with an output class

Object ID	100	100	101	102	102	105	106
Activity	72%	39%	86%	55%	16%	6%	14%
X coordinate	91.81	147.08	122.32	149.07	94.54	156.00	122.17
Y coordinate	127.52	123.17	91.17	129.43	124.18	129.00	91.91
Rotation	2.63	1.98	0.20	0.61	7.60	-3.00	-16.46

The MTO stores most relevant object information: position and orientation. The activity of an identified object is analogous to the pixel activity of structures. As new inputs are applied the activity of previously identified objects either decreases or increases, depending on whether the new input structure has corresponding objects in similar positions or not. Thus, a newly introduced object can be recorded within the MTO, as for example ID 102, 105, and 106 from Table 1. The learning of new objects and the dynamic reconfiguration of the present MTO and structure enable the network to adapt to new inputs. It also allows the network to store most recent information.

The main idea is that the ARTgrid Ga2 module is used as the main information and knowledge system for acquiring and storing all relevant information from the environment. On the other hand, learning will ensure that the system is able to adapt to changing conditions in the environment, acquire them and update the present state. The Ga1 and Ga2 levels of the ARTgrid ANN have very similar architectures. The main difference is in the choice of parameter values that limit the category choice possibilities. Furthermore, each level can be seen as a separate network where the output of Ga1 level records the set of Ga2 level categories within which a more extensive search is conducted. The purpose of the ”dual level” architecture (as shown in Fig. 4) is to enable rapid search through the match tracking process where the best category match needs to be found for a given input structure. An input structure is first recognized at the Ga1 level, and the output neuron that has the highest category choice function is activated. If the resonance value is higher than that of the vigilance parameter, the category is updated with the new input. The same process is repeated for the Ga2 level. If there is no output neuron that yields a resonance level higher than that expected by the vigilance parameter, a new category is formed by storing the input class in a new output neuron, either in Ga1 and Ga2 or only at the Ga2 level. Within the Ga2 level, the initial assembly sequence for the prototype structure is retained. The organization of the network is shown in Fig. 4. Both modules have an additional *Resonance adaptation subsystem* (RAS) that is functioning within each step of the category choice and match tracking. RAS is used for the additional control of category choices. RAS takes into account the object matrix (MTO) and controls the additional resonance gain that can either increase or decrease the resonance value based on the object matrix matching. This process ensures that stable output categories are created both in Ga1 and Ga2. The RAS mechanism is explained in the following section.

An input structure, as shown in Fig. 4, is acquired and passed to the $Ga1_0$ level. In parallel, object information is coded within a separate layer, the object matrix (MTO), which is then passed to the MTO check function. The initial $Ga1_0$ structure acquired by the network is transformed through a shadowed layer [26], adding a proportion of ”blur” around the object contours where a transformed $Ga1_1$ structure is initialized. Blur is added mainly for two reasons. First, uncertainty is present within the localization and recognition process. Possible errors in localization can be compensated by a slight amplification of object contours.

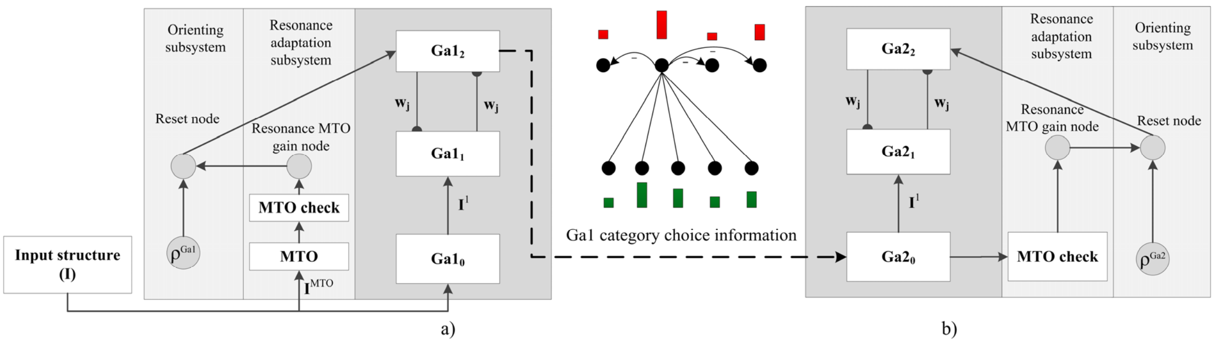

Fig. 4 a) ARTgrid Ga1 module whose category choice is passed to the Ga2 module b) ARTgrid Ga2 module

The modified contours take into account the imperfection of visual object recognition, where visual recognition of objects can be carried out with standard algorithms [27]. Second, as there are multiple objects within the workspace being recognized within a single spatial structure, their relative positions and orientations can vary. The transformed object contours are used for capturing a larger portion of objects that are in different positions and orientations from the initial ones. The input structure **I** is transformed into $\mathbf{I}^1$ given (4).

$$\mathbf{I}_{ij}^1 = \begin{cases} \mathbf{I}_{ij} \ \ \forall \mathbf{I}_{ij} \neq 0 & \\ \mathbf{I}_{ij} b^k, k = \{1,2\} \ \ \forall l_1 + l_2 < l_{\max} & \begin{array}{l} l_1 = \left| i^1 - i \right| \\ l_2 = \left| j^1 - j \right| \end{array} \end{cases} \tag{4}$$

The transformation is done in predefined $l_{\max}$ steps with a transformation function b^k, either linear or quadratic, as noted in (5). Intensity decrease is governed by the value of parameter $\alpha \in [0,1]$. In each iteration an initialization step is made: $\mathbf{I} \leftarrow \mathbf{I}^1$.

$$b^k = \begin{cases} \dfrac{\alpha}{l_1 + l_2} & , k = 1 \\ \dfrac{\alpha}{(l_1 + l_2)^2} & , k = 2 \end{cases} \tag{5}$$

The added blur enables better category match results and also enables the structure morphology to be better merged with the input structure. A related mechanism is utilized within the MTO in terms of object centre elasticity. After the initialization and transformation steps, the input structure situated within the $\mathrm{Ga1}_1$ level is passed through the long-term adaptive connection weights $\mathbf{W}_\mathrm{i}$. A match tracking process is performed, followed by a resonance test as shown in (6).

$$m^{\mathrm{Ga1}} = \frac{\|\mathbf{I} \wedge \mathbf{W}_1\|}{\|\mathbf{I} \vee \mathbf{W}_1\|} \qquad m^{\mathrm{Ga2}} = \frac{\|\mathbf{I} \wedge \mathbf{W}_2\|}{\|\mathbf{I} \vee \mathbf{W}_2\|} \tag{6}$$

The l_1 norm $\|\cdot\|$ is defined as $\|\mathbf{A}\| = \sum_{i=1}^{m} \sum_{j=1}^{n} |a_{ij}|$. If the resonance value m^{Ga1} is higher than the vigilance level, the category choice is valid; the adaptive long-term pathways are updated with respect to the learning law from (2). In the case of resonance value being lower than the vigilance level, the output neuron is inhibited. The resonance test is repeated for the remaining output neurons in order of match the tracking score. In a parallel process, the MTO check node computes the resonance gain R which is appended to the calculated resonance before entering the *reset node*. If there is no output category that yields a resonance level higher than that defined by the vigilance parameter, a new $\mathbf{Ga1}^{n+1}$ category is formed. The Ga1 category choice activates a field of possible Ga2 categories (Fig. 4b) that need to be tested through the match tracking and resonance mechanisms ($m^{\mathrm{Ga2}} > \rho^{\mathrm{Ga2}}$) analogous to the Ga1 level test. When a category match is found, the MTO and the spatial structure morphology are updated regarding (2).

4.2 Object matrix (MTO)

The main issues of the early development stages of the ARTgrid ANN were the proliferation of categories and unwanted category fusion. These issues arose from the fact that there was no mechanism for individual object recognition within the Ga1 and the Ga2 level. As only the global structure was recognized by the NN, certain morphological features of spatial structures faded through learning and recognition iterations. The final result was that certain objects were unrecognizable within the network and the category redundancy occurred as new categories were formed. By slightly modifying the Ga1 and Ga2 parameters, the results went to the other extreme where input spatial structures fused with unwanted output categories forming low generalization ability categories. By inspecting the network output behaviour, a parallel mechanism called Resonance Adaptation Subsystem was developed to enable more stable outputs. The main assumption is that two spatial structures can be considered similar if their morphologies are similar but also individual objects and their relative positions within the structure vary only to a certain extent. Taking into account this hypothesis, the network also needs to have certain information about individual objects within the spatial structure. An object matrix (MTO) mechanism was developed as a parallel match tracking process. It ensures the finding of spatial structure resemblances at a more detailed level. The MTO consists of identified objects and their respective positions and orientations in the workspace. An actual object matrix is presented in Table 1. Each output category has an associated MTO which can also be modified through time by the learning law from (2). The object matrix check function **mtoc** = $f(\mathbf{W}^{MTO}, \mathbf{I}^{MTO})$ contributes to an increase or a decrease in a specified resonance value, either m^{Ga1} or m^{Ga2}. The mechanism utilizes the previous object information stored within the long-term connection weights $\mathbf{W}^{MTO}$ at the Ga1 or the Ga2 level and the MTO of an applied input structure $\mathbf{I}^{MTO}$. Parameters examined through the RAS and the MTO check are: identical objects percentage at $\mathbf{I}^{MTO}$ and $\mathbf{W}^{MTO}$ ($mtoc_1$), match score of $mtoc_1$ object centres identified within a predefined Euclidian distance ($mtoc_2$). An elasticity function (7) is introduced for calculating $mtoc_2$. When the distance between two identified object centres which are in match decreases, the value of $mtoc_2$ increases. The Euclidian distance between object centres is noted as d. In our experiments the parameter d^{min} was set to 8 pixels and d^{max} to 15 pixels, respectively, providing an initial tolerance gap. These values can be changed during simulations and experiments to provide a wider or a narrower tolerance gap for object elasticity.

$$mtoc_2 = \begin{cases} 1 \;\; \forall d \le d^{\min} \\ \dfrac{2(d^{\min} - d)}{d^{\min}} \quad \forall d^{\min} \le d \le d^{\max} \\ 0 \;\; \forall d \ge d^{\max} \end{cases} \tag{7}$$

Additional parameters $mtoc_3$ and $mtoc_4$ specify the difference between the number of objects in $\mathbf{I}^{MTO}$ and in $\mathbf{W}^{MTO}$. Vector **mtoc**=($mtoc_1$, $mtoc_2$, $mtoc_3$, $mtoc_4$) is further multiplied by a 4-dimensional weight vector $\mathbf{v}^{\mathrm{Ga1}}$ or $\mathbf{v}^{\mathrm{Ga2}}$. The calculated output $r = \mathbf{mtoc} \cdot \mathbf{v}^{\mathrm{Ga1}}$ is applied as a resonance gain of the previously calculated m^{Ga1} and m^{Ga2}. The weight vector adds defined contributions for each of the calculated **mtoc** values by a different proportion in the Ga1 and the Ga2 level. Resonance value m^{Ga1} or m^{Ga2}, previously calculated in the resonance check from structure morphology (6), can either be increased or decreased by a defined value within the interval of [-30%, 30%] of the remaining resonance gap. In conducted experiments this value showed a fairly good result but it is not excluded that other values could be used. If a match between objects from the input structure $\mathbf{I}^{MTO}$ and the object information stored within the Ga1 or the Ga2 level ($\mathbf{W}^{MTO}$) is substantial, then the resonance gain r provides a positive correction of the previous resonance value.

5. Simulation and results

Simulations were conducted to test the developed ARTgrid network for a variety of input spatial structure set scenarios. The simulations were performed in MATLAB 2013a on a 3.4 GHz dual-core processor with 4 GB of RAM. In actual applications, the assembly sequence and associated spatial structures will be obtained by visual demonstration from the autonomous agent as described in Fig. 2. A random generator was used to generate discrete sets of input structures. Parameters included in the random generator were the position and orientation of individual objects and their scales. The scales of individual objects were changed within the limits of ±15%. Furthermore, the total number and type of objects in individual structures were altered. Four distinctive objects, as shown earlier in Fig. 2, were used forming different spatial structures. These objects can be seen as symbolic representations of more complex objects. A classification example of 45 randomly generated spatial structures is depicted in Fig. 5.

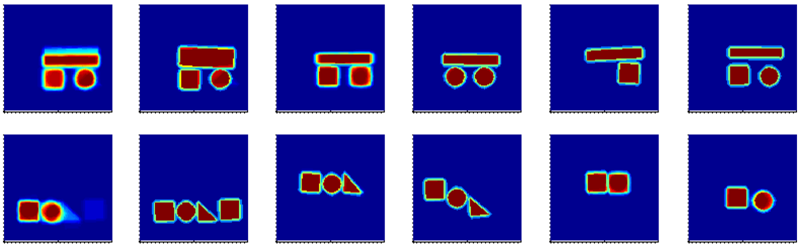

Fig. 5 Classification of 45 spatial structures in two Ga1 categories and five Ga2 categories

In the first column, the main Ga1 category is displayed. Next to each Ga1 category, all respective Ga2 categories are indicated. The parameters were set to: $\beta^{Ga1} = 0.1$, $\beta^{Ga2} = 0.08$, $\rho^{Ga1} = 0.58$ and $\rho^{Ga2} = 0.81$. The leftmost columns in Fig. 5 depict the Ga1 level structures. Continuing to the right, a certain number of Ga2 categories can be observed. The generated input image is 200×200 pixels in size. An individual pixel has a continuous activity level.

The robot is assumed to utilize an incremental learning strategy where neither the input data nor the input sequence is known a priori. For each of the four simulation series a set of 22, 45, 73, and 111 spatial structures were chosen respectively. For each series, 10 simulation runs were conducted (in total 40 simulations). In each simulation run a random sequence of the applied inputs was made.

5.1 Category choice match for the learned patterns

One of the main issues of incremental learning is catastrophic forgetting [28]. In the process of learning new patterns, there is a possibility that they interfere with the already stored patterns. This drawback causes the network to “forget” certain inputs that were applied in previous learning phases. There is no possibility to find the exact category match when a previously presented input is applied again. Our main assumption is that the robot equipped with a learning model based on ARTgrid will not be able to learn in multiple iterations regularly. It will acquire knowledge incrementally. The network should be able to provide stable output results in terms of the inputs that the robot will acquire through visual interaction with the environment. An ideal result would be 100% category choice matches for the already learned patterns. This could be plausible if vigilance parameters ρ^{Ga1} and ρ^{Ga2} are set to a very high value (>0.95). In this way, the category prototype vectors will match only a small number of input structures. Category proliferation will occur where new categories (output classes) are created for a large majority of inputs. The main problem with category proliferation is that the robot information and the learning system will have specific output categories in Ga1 without a sufficient number of Ga2 categories. The search process in the first match tracking phase will be substantially prolonged causing a side effect of delays in the robot reasoning system. Also, the generalization possibility will be weaker compared with the outputs generated by the network having lower values of vigilance parameters as depicted in Fig. 5. This can be a major issue when the robot is confronted with novel but similar stimuli. As the vigilance levels are set high for both Ga1 and Ga2, the new input is rarely recognized as an existing output class, and new categories are formed more often. For this reason a balanced ratio between the generalization and the retrieving of already learned patterns needs to be provided.

Results of category choices and catastrophic forgetting can be seen from the diagrams in Figs. 6 and 7. The results show the effectiveness of the developed network in remembering the already learned patterns. In addition, the cluster centre seeking (CCS) algorithm was applied to the input structure set. CCS is used for the purpose of comparing and validating the results of the ARTgrid model incremental learning strategy. A modified CCS algorithm proposed in [26] is utilized. It uses relative dissimilarity of input structures to find the most distinct input patterns. On average, 10%-15% of input structures are set as cluster centres and are applied to the network initially. The remaining set of input structures is applied in random order. The CCS approach is in contrast with our hypothesis that the learning algorithm cannot have the information of inputs and their sequence in advance. The CCS algorithm is mainly utilized to validate the results generated by the incremental learning strategy of ARTgrid. Fig. 6 presents the results without the CCS Fig. 7 the results with the CCS algorithm applied.

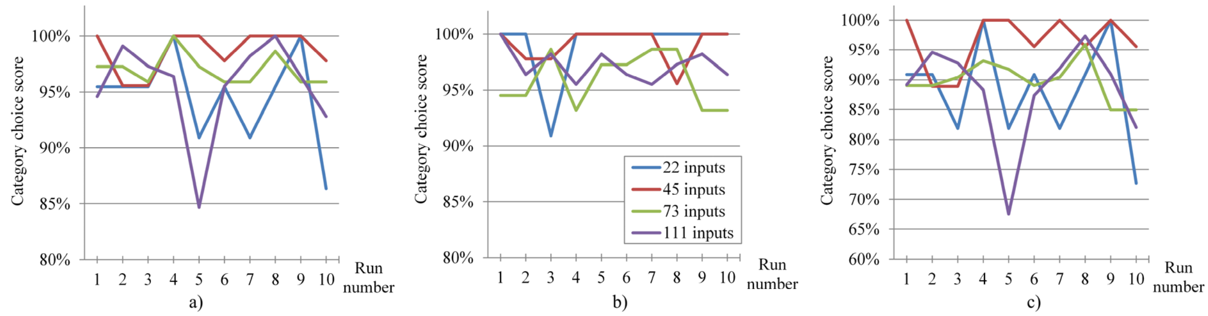

Fig. 6 Category choice score for learned patterns after the first learning iteration (CCS is not applied) a) Ga1 level b) Ga2 level c) both levels

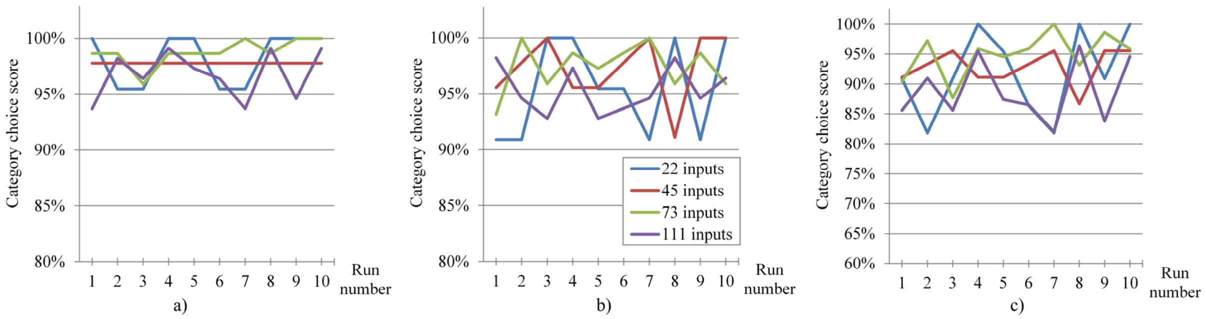

Fig. 7 Category choice score for learned patterns after the first learning iteration (CCS is applied) a) Ga1 level b) Ga2 level c) both levels

The category choice score is defined as the success rate of recognizing the previously learned input patterns (spatial structures) which were applied in the first learning iteration. In the test phase, the network is applied with $\beta^{Ga1}=0$, $\beta^{Ga2}=0$. Only a test match is conducted. The score depicted in Figs. 6a and 7a is computed as the ratio of the Ga1 category match as from the first learning iteration and the total number of inputs applied. On the other hand, the score from Figs. 6b and 7b depicts a category match for the Ga2 level (Ga2 level is compared). Figs. 6c and 7c show the total category match score where both the Ga1 and the Ga2 level are compared with all applied inputs. It can be seen that when CCS is not applied there are certain outliers, i.e. the effect of the random input sequence is more significant. In Section 5.3, a simulation scenario for learning in multiple iterations is conducted.

5.2 Input sequence impact on the Ga1 and the Ga2 category number

The classification of ARTgrid is prone to produce a slight variety in output categories when different sequences of input structures are applied as the input structures are not known in advance (neither their morphologies nor their numbers and other parameters). The number of created categories varies both at the Ga1 and the Ga2 level. This output is expected as the network does not have structured inputs but it learns and updates its long-term connection weights incrementally. In the case where the robot, i.e. its learning model, does not have an a priori view of the world, the sequence of input patterns is arbitrary.

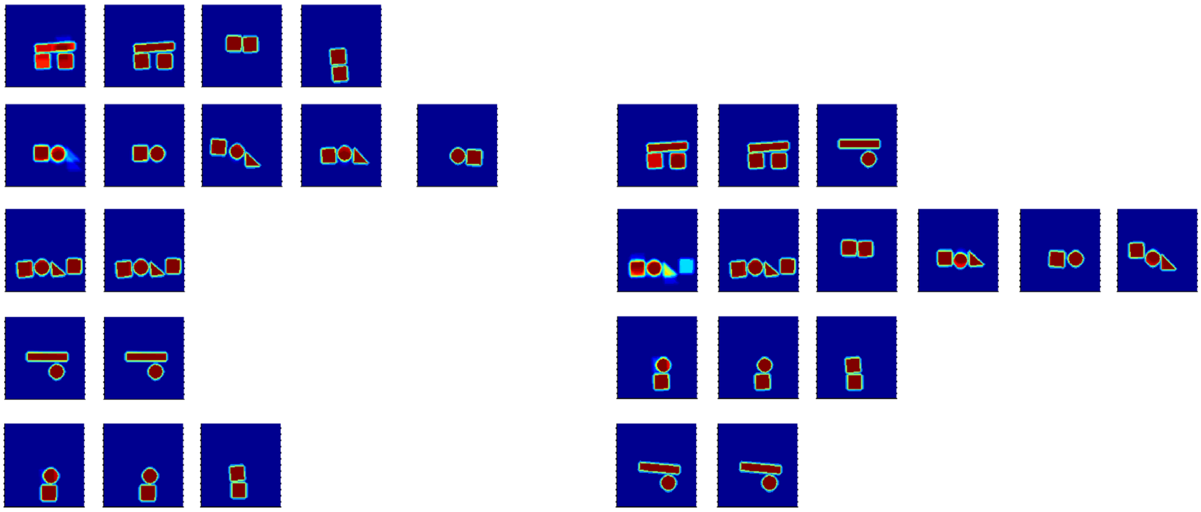

a) b)

Fig. 8 A comparison between two sets of output classes (a and b) from an identical input set of data. The first column represents the Ga1 categories and the respective Ga2 categories are located next to the parent Ga1 category.

To simulate this scenario, each set of input data was generated in a random sequence for each of the 10 simulation runs. Long-term connection weights update, for both the structure morphology and MTO, was done in a single iteration. In each of the 10 simulation runs, a slightly different set of output categories is generated. An example is shown in Fig. 8 where an identical set of input structures was applied to the network in a random sequence.

It can be perceived that the difference between output categories is not substantial. The main issue comes from the order of input samples that generate a different parent Ga1 architecture. By inspecting the network Ga2 classes, it can be concluded that there is only a minor difference between output categories. More detailed results can be observed from Tables 2-4, where the CCS algorithm was used for comparing the results generated by the incremental learning strategy of ARTgrid. The data sets from previous simulations (Figs. 6 and 7.) were used. Results are presented for a single iteration learning scenario.

Table 2 Difference in the Ga1 category number Count-Ga1 (CG1)

ID	No. Inputs	No. runs	$\bar{x}$		max (CG1)		min (CG1)		$\tilde{x}$		σ_{CG1}	
			CCS=1	CCS=0	CCS=1	CCS=0	CCS=1	CCS=0	CCS=1	CCS=0	CCS=1	CCS=0
1	22	10	5	4.3	5	5	5	4	5	4	0	0.48
2	45	10	5	5.5	5	7	5	4	5	5	0	0.97
3	73	10	6	4.8	6	6	6	4	6	5	0	0.63
4	111	10	7	6.7	7	7	7	6	7	7	0	0.48

Table 3 Difference in the Ga2 category number Count-Ga2 (CG2)

ID	No. Inputs	No. runs	$\bar{x}$		max (CG2)		min (CG2)		$\tilde{x}$		σ_{CG2}	
			CCS=1	CCS=0	CCS=1	CCS=0	CCS=1	CCS=0	CCS=1	CCS=0	CCS=1	CCS=0
1	22	10	9.4	10.4	10	12	9	9	9	10	0.52	1.07
2	45	10	19.1	19.6	20	21	18	17	19	20	0.74	1.35
3	73	10	15	14.8	15	17	15	13	15	14	0	1.40
4	111	10	19.5	20.5	21	23	18	17	19.5	20.5	0.85	1.90

Table 4 Difference in the total (Ga1+Ga2) category number; total count-Ga1, Ga2 (CGT)

ID	No. Inputs	No. runs	$\bar{x}$		max (CGT)		min (CGT)		$\tilde{x}$		σ_{CGT}	
			CCS=1	CCS=0	CCS=1	CCS=0	CCS=1	CCS=0	CCS=1	CCS=0	CCS=1	CCS=0
1	22	10	14.4	14.7	15	17	14	13	14	14.5	0.52	1.34
2	45	10	24.1	25.1	25	27	23	22	24	25	0.74	1.37
3	73	10	21	19.6	21	22	21	18	21	19.5	0	1.43
4	111	10	26.5	27.1	28	30	25	23	26.5	27	0.85	1.91

The results from Tables 2-4 show the mean value $\bar{x}$ of output category number, the maximum and minimum numbers of formed categories, the median $\tilde{x}$, and the standard deviation σ. The set of all simulation runs conducted with the CCS (CCS=1) algorithm applied will be denoted as $\mathcal{S}_1$ while the set where CCS is not applied (CCS=0) will be denoted as $\mathcal{S}_2$. It can be observed that there is a good match $\Delta = \bar{x} - \tilde{x}$ between the mean and the median for all cases, with a slightly better result in $\mathcal{S}_1$. Furthermore, a more stable category number and hierarchy are achieved compared to network outputs in $\mathcal{S}_2$. On average, σ is 65% lower, indicating more compact output groups within $\mathcal{S}_1$. By taking into account that the network had information of all inputs in advance, a better result was expected. If the deviation of the total number of categories is observed, on average, the outputs generated in $\mathcal{S}_2$ produced an increase in 17% of categories in total ($\sum$(Ga1,Ga2)) with respect to $\mathcal{S}_1$. If we take into consideration that ~12.5% of inputs were allocated for CCS and applied initially to the network, no marked positive effect of the cluster centre seeking algorithm can be observed. The main factor that gives rise to the total category number in $\mathcal{S}_2$ is the effect of random input sequence and the winner-take-all (WTA) strategy. When CCS is applied, the network is initiated with the most distinctive and dissimilar input structures providing a better starting category set $\mathcal{B} \subset \mathcal{S}_1$ through which all further inputs could be recognized and categorized. Consequently, there is a weaker possibility that specific categories, after a certain time, get unused, i.e. that some newly formed output category provides better generalization and recognition capabilities. Taking into consideration the assumption that the network, i.e. the robot, will use an incremental learning strategy, the possibility of creating different virtual maps of the world corresponding to different input sequences is acceptable.

5.3 Multiple iteration learning

A category match stability test is conducted assuming that the network confronts an identical or very similar input multiple times after its first learning cycle. The category choice score (Fig. 9) is defined as the success rate of recognizing the learned input patterns (spatial structures) which were applied in the previous learning iteration. The result of applying an identical set $\mathcal{S}_2$ of inputs in a random sequence through a number of iterations is displayed. The network parameters were set to: $\beta^{Ga1} = 0.1$, $\beta^{Ga2} = 0.08$, $\rho^{Ga1} = 0.58$ and $\rho^{Ga2} = 0.81$. A category match of 97% is achieved after the second learning iteration compared to 88.5% match score in a single iteration learning process. The network reaches stability (Category choice score >98%) after the sixth learning iteration. $\mathcal{S}_2$ was applied in multiple iterations and CCS was not initiated. The results in Fig. 9 are given for a random set of inputs. It can be observed that the increase in the category match score has a maximum rate in sequences with a smaller sample size (22 and 45 input structures) where stability is reached in a lower number of learning iterations.

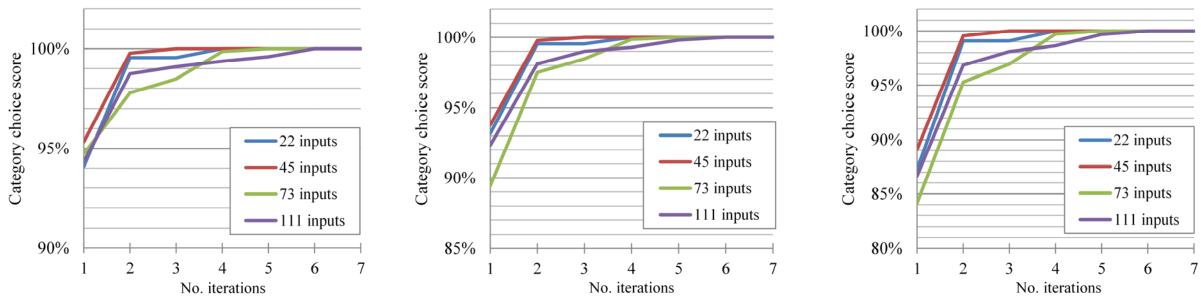

a) b) c)

Fig. 9 Category choice score for learned patterns in multiple iteration learning a) Ga1 level b) Ga2 level c) Total category choice score (Ga1 and Ga2 levels) for learned patterns in multiple iteration learning

6. Discussion and conclusion

The main purpose of the learning architecture is to enable the robot to classify spatial structures and also to generalize the associated knowledge. One important feature of the ARTgrid network is the ability to categorize by creating related generic structure classes. The vigilance parameters at the Ga1 and the Ga2 level control the similarity of inputs and established categories within the ARTgrid network. As mentioned earlier, both the MTO and the morphology of the spatial structures are updated with respect to the learning laws. A mechanism for resonance adjustment (adaptation) through MTO matching was proposed.

A simulation demonstrating the use of CCS algorithm in a single iteration learning scenario was shown in Figs. 6 and 7. The category choice match for the learned patterns in $\mathcal{S}_1$ is on average 1.8% higher than the results obtained when $\mathcal{S}_2$ is applied. In conclusion, by utilizing the CCS algorithm, classification capabilities are not significantly altered. The effect of the remaining input structures that are not applied through CCS (85% - 90% of remaining inputs) is very similar because they are applied in random sequence. What CCS enables is a better dissipation of starting categories that provide the network with more stable outputs as can be observed from Figs. 6 and 7. In 5% of simulation runs, the category choice match for learned patterns was substantially low ($\mathcal{S}_2$) with a score of 68% and 73%, while all other scores were higher than 80 %. When $\mathcal{S}_1$ is applied, a more stable output is maintained, where the output score stabilizes at a constant rate of above 80% in all 40/40 simulation runs. A more marked effect of applying CCS can be seen within the total category number dissipation, within both the Ga1 and the Ga2 level, as can be seen from Tables 2 - 4. Maximum span in the category numbers is compared. When CCS was applied there was a more stable output generated by the network where the total difference in category numbers (see Table 4) was in a range 0-3 ($\bar{x}$ = 1.5). In comparison, the output of the network without applying CCS had a larger variety in category numbers: total difference in the category numbers was in the range 4-7 ($\bar{x}$ = 5). Furthermore, simulation results have provided an answer to how close in terms of similarity the results of ARTgrid are in relation to different representations of the identical stimuli. In terms of single iteration learning, where inputs cannot be structured or known in advance, the average match score of 88.5% was achieved. The percentage of previously learned structures that the network "forgets", i.e. that are either recognized within another category or a new category is formed, was 11.5%.

More extensive tests were done by applying previously learned patterns in a multiple iteration learning scenario to test whether the network stabilizes its outputs. By inspecting the category choice score in diagrams from Fig. 9, a positive trend of match score increase can be observed in the process of multiple iteration learning. An average match score higher than 95% was obtained at the end of the second learning cycle. While at the end of the sixth learning cycle, all match scores stabilized at >98%.

7. Future work

In perspective, an active memory search process should be developed. An additional bottom-up approach is planned for the ARTgrid network. The current model can find similarities between the input structure morphology and an existing category. The ARTgrid variant model will be developed for finding similarities between object matrices as the primary matching mechanism.

Utilizing the capability of socket messaging as a standard communication interface, the ARTgrid network will be used for controlling an industrial 6 DOF robot arm within the previously developed framework [29]. In future research which will include the implementation on actual robotic equipment, the general model will be illustrated in more detail. Furthermore, the capability of 3D interpretation of spatial structures will be investigated.

ACKNOWLEDGEMENT

Authors would like to acknowledge the support of the Croatian Scientific Foundation through the research project ACRON - A new concept of Applied Cognitive RObotics in clinical Neuroscience.

REFERENCES

[1] M. Švaco, B. Jerbić, and F. Šuligoj, "ARTgrid: A Two-Level Learning Architecture Based on Adaptive Resonance Theory," *Adv. Artif. Neural Syst.*, vol. 2014, pp. 1–9, 2014.

[2] S. Grossberg, "Adaptive Resonance Theory: How a brain learns to consciously attend, learn, and recognize a changing world," *Neural Netw.*, vol. 37, pp. 1–47, Jan. 2013.

[3] G. A. Carpenter and S. Grossberg, "Adaptive Resonance Theory," in *Encyclopedia of machine learning*, Springer, 2011.

[4] A. Weitzenfeld, *The neural simulation language: a system for brain modeling*. Cambridge, MIT,2002.

[5] C. Heyer, "Human-robot interaction and future industrial robotics applications," in *Intelligent Robots and Systems (IROS), 2010 IEEE/RSJ International Conference on*, 2010, pp. 4749–4754.

[6] V. R. Kompella, M. Luciw, M. Stollenga, L. Pape, and J. Schmidhuber, "Autonomous learning of abstractions using curiosity-driven modular incremental slow feature analysis," in *Development and Learning and Epigenetic Robotics (ICDL), 2012 IEEE International Conference on*, 2012, pp. 1–8.

[7] T. Stipančić, B. Jerbić, and P. Ćurković, "Context-Aware System Applied in Industrial Assembly Environment," *Int. J. Adv. Robot. Syst.*, p. 1, 2012.

[8] P. Ćurković, B. Jerbić, and T. Stipančić, "Coordination of Robots with Overlapping Workspaces Based on Motion Co-evolution," *Int. J. Simul. Model.*, vol. 12, no. 1, pp. 27–38, doi:. .2507/IJSIMM12(1)3.222 2013.

[9] A. Bannat, T. Bautze, M. Beetz, J. Blume, K. Diepold, C. Ertelt, F. Geiger, T. Gmeiner, T. Gyger, A. Knoll, C. Lau, C. Lenz, M. Ostgathe, G. Reinhart, W. Roesel, T. Ruehr, A. Schuboe, K. Shea, I. Stork genannt Wersborg, S. Stork, W. Tekouo, F. Wallhoff, M. Wiesbeck, and M. F. Zaeh, "Artificial Cognition in Production Systems," *IEEE Trans. Autom. Sci. Eng.*, vol. 8, no. 1, pp. 148–174, Jan. 2011.

[10] H. Ogata, M. Tsuda, and M. Mizukawa, "Teaching 6-DOF tasks for robot operating assembly in the same category," 1997, pp. 693–698.

[11] G. V. Paul, Y. Jiar, M. D. Wheeler, and K. Ikeuchi, "Modelling human assembly actions from observation," 1996, pp. 357–364.

[12] D. R. Myers, M. J. Pritchard, and M. D. Brown, "Automated programming of an industrial robot through teach-by showing," 2001, vol. 4, pp. 4078–4083.

[13] C. Lenz, S. Nair, M. Rickert, A. Knoll, W. Rosel, J. Gast, A. Bannat, and F. Wallhoff, "Joint-action for humans and industrial robots for assembly tasks," 2008, pp. 130–135.

[14] C. Lenz, "Context-aware human-robot collaboration as a basis for future cognitive factories," Technische Universität München, 2011.

[15] M. Rickert, M. E. Foster, M. Giuliani, T. By, G. Panin, and A. Knoll, "Integrating language, vision and action for human robot dialog systems," in *Universal Access in Human-Computer Interaction. Ambient Interaction*, Springer, 2007, pp. 987–995.

[16] D. C. Wunsch, "ART properties of interest in engineering applications," 2009, pp. 3380–3383.

[17] E. Berghöfer, D. Schulze, C. Rauch, M. Tscherepanow, T. Köhler, and S. Wachsmuth, "ART-based fusion of multi-modal perception for robots," *Neurocomputing*, vol. 107, pp. 11–22, May 2013.

[18] S. S. Seyhan, F. N. Alpaslan, and M. Yavaş, "Simple and complex behavior learning using behavior hidden Markov model and CobART," *Neurocomputing*, vol. 103, pp. 121–131, Mar. 2013.

[19] I. Lopez-Juarez and M. Howarth, "Learning manipulative skills with art," in *Intelligent Robots and Systems, 2000.(IROS 2000). Proceedings. 2000 IEEE/RSJ International Conference on*, 2000, vol. 1, pp. 578–583.

[20] L. Gu and J. Su, "Humanoid Robot Behavior Learning Based on ART Neural Network and Cross-Modality Learning," in *Advances in Natural Computation*, vol. 4221, L. Jiao, L. Wang, X. Gao, J. Liu, and F. Wu, Eds. Berlin, Heidelberg: Springer Berlin Heidelberg, 2006, pp. 447–450.

[21] P. K. Park, J. H. Lee, C. W. Shin, H.-S. Ryu, B.-C. Kang, G. A. Carpenter, and S. Grossberg, "Gesture recognition system based on Adaptive Resonance Theory," in *Pattern Recognition (ICPR), 2012 21st International Conference on*, 2012, pp. 3818–3822.

[22] W. Fung and Y. Liu, "Adaptive categorization of ART networks in robot behavior learning using game-theoretic formulation," *Neural Netw.*, vol. 16, no. 10, pp. 1403–1420, Dec. 2003.

[23] A.-H. Tan, G. A. Carpenter, and S. Grossberg, "Intelligence through interaction: Towards a unified theory for learning," in *Advances in Neural Networks–ISNN 2007*, Springer, 2007, pp. 1094–1103.

[24] M. Švaco, B. Šekoranja, and B. Jerbić, "Autonomous Planning Framework for Distributed Multiagent Robotic Systems," in *Technological Innovation for Sustainability*, Springer, 2011, pp. 147–154.

[25] G. A. Carpenter, S. Grossberg, and D. B. Rosen, "Fuzzy ART: Fast stable learning and categorization of analog patterns by an adaptive resonance system.," *Neural Netw.*, vol. 4, no. 6, pp. 759–771, 1991.

[26] B. Jerbić, "Autonomous robotic assembly using collaborative behavior based agents," *Int. J. Smart Eng. Syst. Des.*, vol. 4, no. 1, pp. 11–20, 2002.

[27] T. Urbancic, M. Kosmatin Fras, and B. Stopar, "The Influence of the Input Parameters Selection on the RANSAC Results," *Int. J. Simul. Model.*, vol. 13, no. 2, pp. 159–170, Jun. 2014.

[28] Motonobu Hattori, "Avoiding Catastrophic Forgetting by a Biologically Inspired Dual-Network Memory Model," vol. 7664, Springer Berlin Heidelberg, 2012.

[29] M. Švaco, B. Šekoranja, and B. Jerbić, "Industrial Robotic System with Adaptive Control," *Procedia Comput. Sci.*, vol. 12, pp. 164–169, Jan. 2012.

Submitted: 17.09.2014

Accepted: 10.12.2014

Marko Švaco*
Bojan Jerbić
Filip Šuligoj
Faculty of Mechanical Engineering and
Naval Architecture,
University of Zagreb
Ivana Lučića 5, 10000 Zagreb, Croatia
*marko.svaco@fsb.hr